Title	Mechanical Properties on Electron Beam Welds of Constructional High Tension Steels (Report III)
Author(s)	Arata, Yoshiaki; Matsuda, Fukuhisa; Shibata, Yutaka et al.
Citation	Transactions of JWRI. 4(2) p.181-p.187
Issue Date	1975-10
oaire:version	VoR
URL	https://doi.org/10.18910/11120
rights	
Note	

Mechanical Properties on Electron Beam Welds of Constructional High Tension Steels (Report III) †

Yoshiaki ARATA*, Fukuhisa MATSUDA**, Yutaka SHIBATA***, Shigeomi HOZUMI***
Yoshihisa ONO*** and Shouichiro FUJIHIRA****

Abstract

In this investigation, the authors aimed to make clear the weldability of electron-beam welds for some commercial constructional high tension steels. Then, the influence of weld heat input on the weld defects, the hardness distributions and the impact properties of the electron-beam welds was investigated in this report. The materials used were three grades of high tension steel HT50, HT60 and HT80 with 25 mm thickness. The conventional low voltage type electron-beam welder, 30 KV-500 mA(15 KW) in maximum was employed in this experiment.

All of weld bead were performed with bead-on-plate type welding. The active beam parameter, a_b adopted was 1.0 through the experiment.

The remarkable conclusions are as follows:

(1) *All of weld seam except unstable location of bead have had no defect according to dye penetrant and X-ray inspections.*
(2) *The hardness in weld metal was generally reduced with an increase of weld heat input. In Vickers hardness distributions of HT50 and 60 steels, the hardness in the HAZ near fusion boundary was harder than that in the weld metal. This is considered due to the vaporization of Mn element in weld metal.*
(3) *The value of impact strength for weld metal usually showed the different two levels, lower and higher, at particular testing temperature due to the difference in the fracture mode for 2 mm notched standard Charpy impact test specimen. Namely, when the fracture occurred straightly along the notched direction, the absorbed energy showed lower value, however, when the fracture occurred out of the notched direction, it showed higher value.*
(4) *The particular testing temperature, at which the fracture mode differs, tended to be raised with an increase of the weld heat input. This seemed to be related with the bead width of fusion zone and the hardness difference between base and weld metal.*
(5) *As far as the fracture propagates along the notched direction, there is little variation in the absorbed energies of weld metal for respective material within a limited change for the weld heat input from 10 KJ/cm through 40 KJ/cm.*
(6) *In case of the welds of HT50 and 80 steels, the absorbed energies of the weld metal, which show lower value than that of the base metal are usually exceeding the minimum absorbed energy required in JIS or WES specification, even though the fracture occurs within weld metal. In case of HT60, however, they are not always satisfied with the criteria of JIS specification.*
(7) *Furthermore, the impact strength of electron-beam welds showed higher value than that of submerged arc welds for HT50 and 80 steels.*

1. Introduction

There are few data concerning the mechanical properties on electron-beam welds of the constructional high tension steels (HT50, 60 and 80 steels) which are used in large-sized constructions, and its weldability is still unknown. Then, in this investigation the authors aimed to make clear them.

Some results of the mechanical properties of electron-beam welds such as hardness distribution, tensile, bend, impact and fatigue properties were reported in the two previous reports.[1],[2] It was recognized that the results of these mechanical tests except some impact properties of HT50 steel would be satisfied with the practical use for many fields of application.

Then, in this report, the authors mainly treated about the more detailed behavior of impact properties for electron-beam welds, which were characterized by narrow bead width as compared with that of the welds by conventional arc welding method. Namely, the influence of the weld heat input on the impact properties of weld metal was investigated, and it was discussed that the behavior of impact properties of electron-beam welds is closely related to both the bead width and the hardness difference between base and weld metal.

† Received on July 29, 1975
* Professor
** Associate Professor
*** Katayama Iron Works, Ltd.
**** Co-operative Researcher (1975), Katayama Iron Works, Ltd.

2. Materials and Welding Conditions

The materials used in this investigation are HT50, 60 and 80 steels which are widely used in the constructional bridges and buildings. The chemical compositions of these three types of high tension steels are listed in Table 1. The carbon equivalent (C_{eq}) of HT 50, 60 and 80 steels is 0.37,0.36 and 0.50, respectively. All of the plate thickness of these steels are 25 mm.

High vacuum type-EB welder, conventional low voltage type (30 KV-500 mA, 15 KW in maximum), was used in this investigation. The welding conditions used on various materials are tabulated in Table 2. The weld heat input is varied for the different four levels from 10

Table 1 Chemical composition of HT50, 60 and 80 steels used.

Composition / Steel	C	Si	Mn	P	S	Ni	Cr	Mo	V	Ceq*
HT50 (SM50)	0.14	0.46	1.27	0.023	0.020	–	–	–	–	0.37
HT60 (SM58)	0.12	0.35	1.16	0.018	0.010	0.02	0.10	–	0.030	0.36
HT80	0.13	0.29	0.85	0.016	0.008	0.98	0.48	0.39	0.023	0.50

*: Ceq = C + 1/6Mn + 1/24 Si + 1/40 Ni + 1/5 Cr + 1/4 Mo + 1/14 V

(JIS G 3106)

through 40 KJ/cm. the welding for all materials was performed with one pass bead-on-plate welding method. In case of the welding conditions, (c) and (d), in which 25 mm thick steel plates were burnt through, the welding was performed by means of the stacking of respective two plates.

In this experiment, the focal length of electron-beam was beforehand certified by the slope-welding method[3] and the active beam parameter, a_b was selected for 1.0. The focal length (D_F) of each welding condition was shown on the right part of Table 2. The size of each specimen is 150 mm in width and 500 mm in length. Any oxide and scaling on the plate surfaces was completely machined.

3. Experimental Results

3.1 Defect of welds

All of the electron-beam welds of high tension steels were X-ray inspected. The defects such as porosity and crack could not be particularly detected in the electron-beam welds of HT50, 60 and 80 steels. However, hot cracks were often observed in the crater points, or the places where the electron-beam irregularily stopped. Referring to Japan Industrial Standard Specification (JIS Z 3104-1968), most of the electron-beam welds except irregular points were allowable in the first class for synthetic grade. All of the weld surfaces of the high tension steels were also checked by dye penetrant test. No surface defects were observed at all in them.

Table 2 Welding conditions used.

Designation of welding condition	Beam power (KV-mA)	Welding speed (cm/min)	Weld heat input (KJ/cm)	Focal length (mm)
(a)	30–200 (6KW)	36	10	255
(b)	30–300 (9KW)	36	15	234
(c)	30–400 (12KW)	36	20	218
(d)	30–400 (12KW)	18	40	218

3.2 Metallographic and hardness examinations

Photo. 1 shows the macro-and micro-photographs for HT80 welds in various weld heat inputs from 10

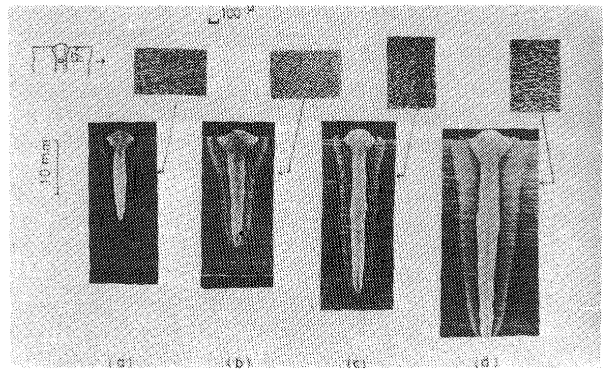

Photo 1 Macro-and microphotographs for HT80 welds in various weld heat inputs.
(a) 10 KJ/cm (b) 15 KJ/cm (c) 20 KJ/cm
(d) 40 KJ/cm

through 40KJ/cm. The micro-photographs indicate the micro-structures of weld metal at 7 mm downwards from the plate surface. The grain size of micro-structure of the weld metal tended to grow coarser with an increase of the weld heat input. This tendency shows irrespective of the difference of materials.

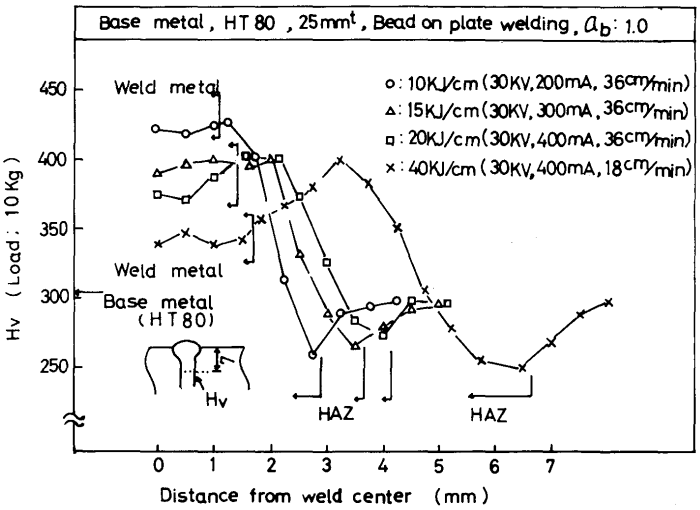

Fig.1 Vickers hardness distributions for HT80 welds in various weld heat inputs.

The hardness of welds was measured by using Vickers hardness tester with 10 Kg load. Vickers hardness distributions of HT80 welds in various weld heat inputs are shown in Fig. 1. The measured points are at 7 mm downwards from surface, which are accordant with the center of impact test specimens adopted. With an increase of the weld heat input, the cooling rate becomes faster and the hardness of weld metal are graduately decreased. Fig. 2 shows an example of the hardness distributions of HT50, 60 and 80 welds, the weld heat input of which is 15KJ/cm.

As mentioned in the previous report, the maximum hardness in HT50 and 60 welds is observed in the HAZ near fusion boundary, which is caused by the vaporization of Mn element in the weld metal during welding. In the welds of HT60 and 80, the softened zones are observed because they are quenched and tempered steels. Fig. 3 shows the relation between the weld heat input and the hardness of welds for HT50, 60 and 80 steels. Hw is the average hardness of weld metal.

H_w tends to be decreased with an increase of the weld heat input regardless of the difference of materials. Especially, the hardnesses in HT80 welds showed remarkably higher value than those in the welds of the other materials. Namely, the degree of hardness in the weld metal is closely related to the value of carbon equivalent in Table 1. Fig. 4 shows the hardness distributions of weld metals inward direction for HT50, 60 and 80 welds in case of 15KJ/cm weld heat input. In HT80 welds, there were no variations in the hardness of weld metal inward direction, while in HT50 and 60 welds, there are obvious differences in the hardness between the surface and bottom part of the bead, and the maximum hardnesses are observed in the tops of spiking in both weld metals. It is considered that these differences in hardness are caused by the difference of the cooling rate between the bead surface and bottom, which is related to the degree of hardness.

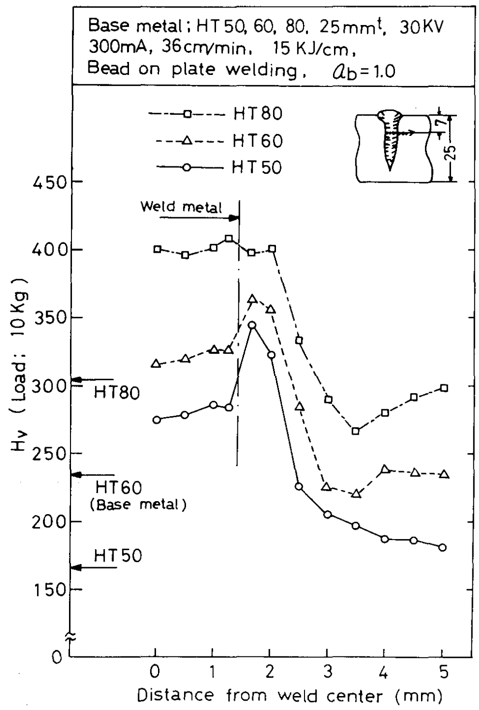

Fig. 2 Vickers hardness distributions of welds for HT50, 60 and 80 steels in 15 KJ/cm weld heat input.

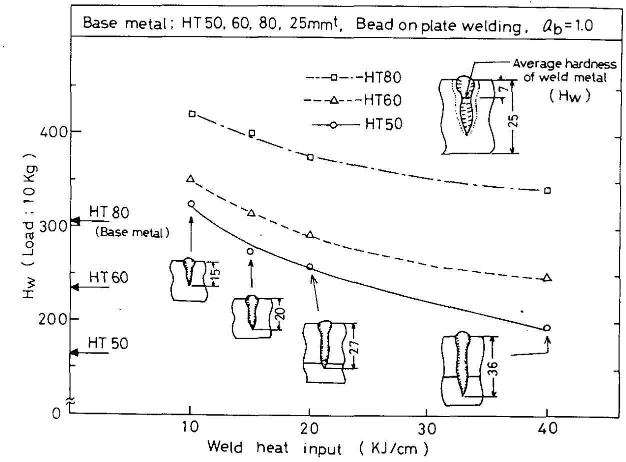

Fig. 3 Relation between weld heat input and average hardness of weld metal for HT50, 60 and 80 steels.

This difference in the degree of hardness due to the difference of materials should be considered by the combination with CCT diagram for respective material.

3.3 Impact properties

Impact test was performed with standard Charpy 2 mm V notch specimens. The capacity of impact test machine is 30 Kg-m in maximum. The test specimens were machined from 2 mm under the plate surface, and all specimens were notched at the center of weld metal. Six levels of testing temperature, –80, –60, –40, –15, 0°C and room temperature (15°C) were selected in this examination and the effects of weld heat input on the impact properties were investigated for HT50, 60 and 80 welds. Usually, two to four test specimens were tested for each testing temperature. As the common phenomenon in impact test for the welds of each materials, it was often observed that the value of impact strength usually showed the different levels even at the same testing temparature, which has already been reported previously. It was due to the difference in the three types of fracture mode for impact test specimens as illustrated in Fig. 5.

Namely, the different fracture mode concurrently occurs at the same testing temperature, and the value of impact strength is varied in response to respective fracture mode. In general, at the lower temperature side of that, the fracture mode ordinarily becomes (A) type, on the

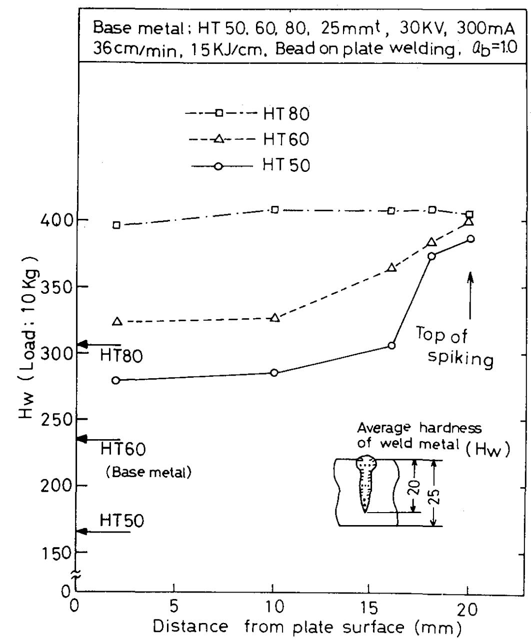

Fig. 4 Vickers hardness distributions of weld metals inward direction for HT50, 60 and 80 steels.

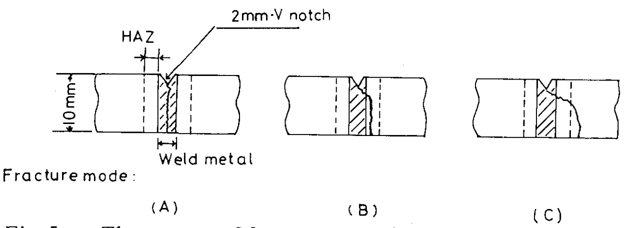

Fig. 5 Three types of fracture mode for impact test specimens.

other hand, at the higher temperature side of that it ordinarily becomes (B) or (C) type. In case of (A) type the fracture occurs straightly along the notched direction, while in case of (B) and (C) types it deviates to HAZ and base metal, respectively. Then as the distance of fracture path is increased in order of type (A), (B) and (C), the absorbed energy of weld metal in case of type (A) shows the lowest value in all of types. Then all of transition curves in this report were shown with the distinction of the type of fracture mode in the tested specimens.

As an example, the transition curve for HT80 welds in 10KJ/cm weld heat input is shown in Fig. 6. It is found that the absorbed energy obviously showed two different values at – 40°C testing temperature due to the difference of the fracture mode. And in the higher temperature than –40°C, the fracture path ordinarily deviated to the base metal and its energy showed remarkably high value, while in the lower temperature it occurs within the weld metal and its energy showed low value. It seems that there is little fluctuation in impact strength for respective fracture mode at the particular testing temperature. As mentioned in the above, it is found that the toughness of the weld metal in itself, which is made

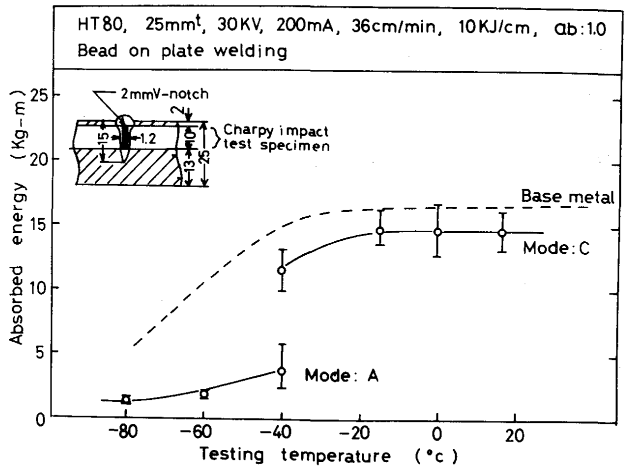

Fig. 6 Transition temperature curve for HT80 welds in 10KJ/cm weld heat input.

clear only at lower testing temperature than –40°C, showed lower value than that of base metal in general. Figs. 7, 8 and 9 show the comparisons of transition curves in various weld heat inputs for HT50, 60 and 80 welds, respectively.

In case of HT50 (Fig. 7), the fracture mode respectively began to separate into two types at –60 and –15°C in 10 and 15KJ/cm weld heat inputs, however it didn't separate even at 20°C in 40KJ/cm. Namely, the transition temperature for the fracture mode tended to shift to higher temperature side with an increase of the weld heat input. However even in the two formers, the test specimens for (A) type fracture mode were observed at about room temperature, and then the impact strength of the weld metal in itself was able to be obtained. Judging from this result, it is found that there is little variation in the impact strength of the weld metal in itself within the changing range of the weld heat input in this investigation, and its value corresponds to that of base metal. The energy transition temperatures for weld metal are about –20°C.

On the other hand, in case of HT60 (Fig. 8), at about room temperature, (A) type-fractured specimens were not observed except in large weld heat input of 40KJ/cm. Furthermore, the transition temperature for the fracture mode has the tendency to shift to higher temperature side with an increase of the weld heat input, which is the same as that of HT50. According to mentioned in the above, the toughness of the weld metal in itself is not clear all temperatures range. However, with the analogy from the impact properties in 40KJ/cm in general its impact strength seems to show lower value than that of base metal. And also it seemed that there is no obvious difference in the impact strength of weld metal due to the variation of weld heat input.

Nextly the result of HT80 welds (Fig. 9) was almost similar to that of HT60. Fig. 10 shows the transition

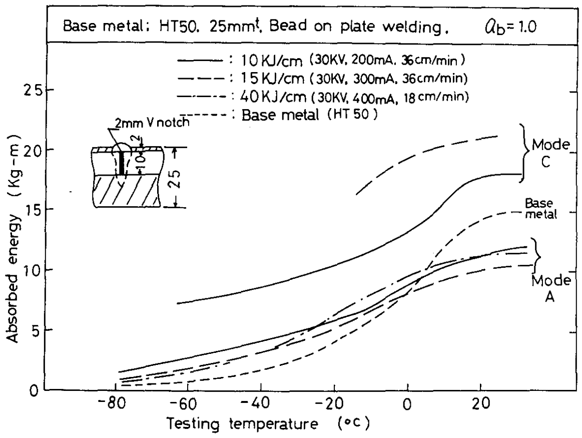

Fig. 7 Comparison of transition temperature curves for HT50 welds in various weld heat inputs.

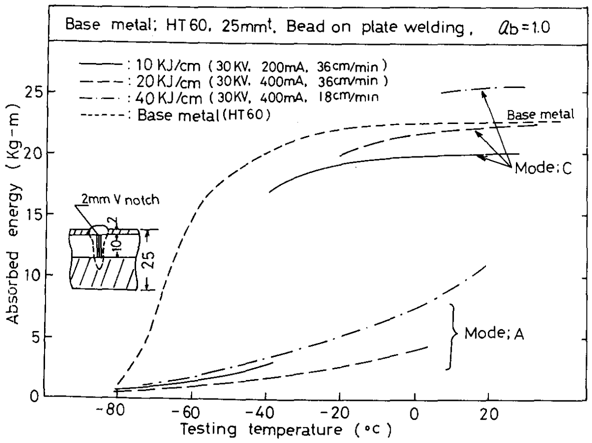

Fig. 8 Comparison of transition temperature curves for HT60 welds in various weld heat inputs.

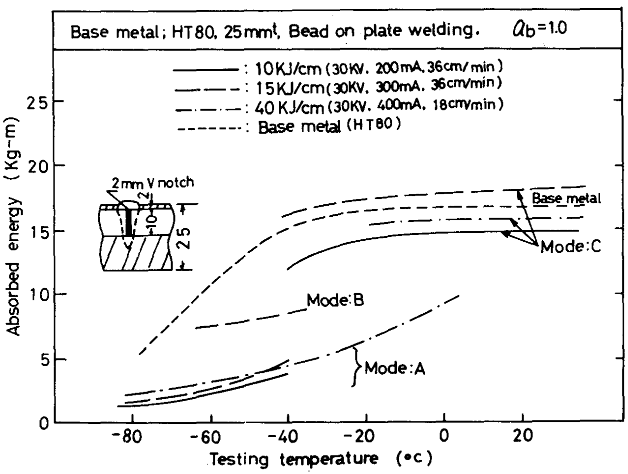

Fig. 9 Comparison of transition temperature curves for HT80 welds in various weld heat inputs.

curves for the submerged arc welds of HT50, 60 and 80 steels, which were asked in order to compare the impact properties of electron-beam welds with those of conventional arc welds. Each material is identical with that used for the electron-beam welding, and the welding conditions used are given in the upper part of Fig. 10. The fracture modes for the tested specimens were all (A) types in Fig. 5. All of the impact strengths showed extremely low

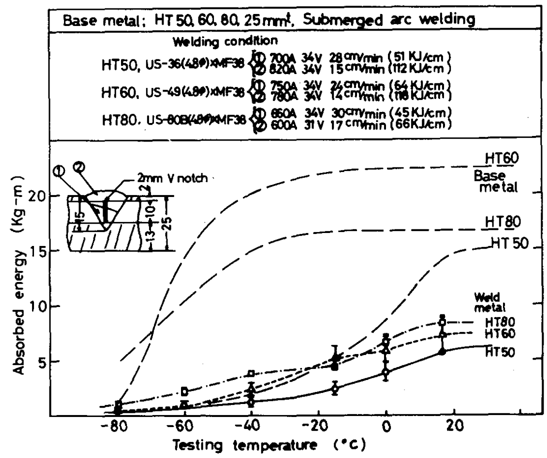

Fig. 10 Transition temperature curves for submerged arc welds of HT50, 60 and 80 steels.

values as compared with repective base metal, which is considered due to a little large weld heat input. And also it is found that there is no obvious difference in the value of the impact strength between the electron-beam and submerged arc welds.

Nextly, the relation existing between the weld heat input and the transition temperature for fracture mode in HT50, 60 and 80 welds is shown in Table 3. Moreover both the bead width (d_B) and the average hardness of weld metal (Hw) at 7 mm downwards from the surface which corresponds to each weld heat input are also listed in the table. Additionally, the bead width ratio, (d_B/h) and the hardness difference ratio, $H_w - H_s/H_s$ are calculated and given, too. h indicates the remained thickness in the bottom of notch for Charpy specimens, which is 8 mm for this case. H_s indicates the hardness in base metal for HT50 or in softened zone for HT60 and 80. In general, regardless of the difference of materials, the transision temperature for fracture mode has the tendency to rise with an increase of the bead width ratio, or with an decrease of the hardness difference ratio. That is, it is found that as the bead width ratio is decreased smaller, and as the hardness difference is increased larger, the fracture for Charpy specimens tends to deviate to the base metal side even at lower testing temperature.

Then, for instance, concerning to HT60 welds in 15KJ/cm weld heat input, the impact properties for the weld metal were examined by means of 5 mm V notched specimens. They were produced by way of trial to have 5 mm V notch to 10 mm square. Fig. 11 shows the impact test results of HT60 welds by using 5 mm V notch specimens. In this instance, as the bead width ratio is increased larger as compared with 2 mm V notch, even at 100°C testing temperature the fracture in this specimen did not deviate to the base metal side, that is, the fracture modes were all (A) types. From this result it is obvious that the transition temperature for fracture mode is influenced by the bead width ratio. And also the value of impact strength becomes constant at 80°C testing temperature, and the energy transition temperature for this curve is about 40°C, which is extremely high as compared with that (about −65°C) of the base metal.

As above-mentioned, it is found that the transition temperature for fracture mode are obviously affected by both the bead width ratio and the hardness difference ratio. However, it is still unknown which ratio between them has more influence on the fracture mechanism. Nextly, Fig. 12 shows the relation existing between the weld heat input and the absorbed energy of weld metal at specified temperature in JIS (Japan Industrial Standard)

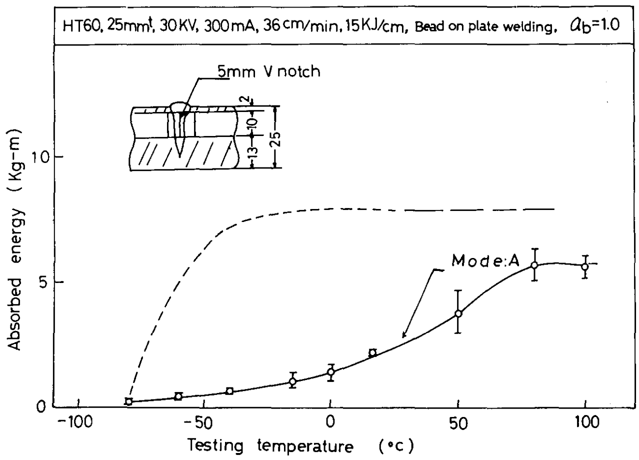

Fig. 11 Impact test results of HT60 welds by using 5mm-Vnotch specimens.

for HT50 and 60, or in WES (Japan Welding Standard) Specification for HT80. According to these specifications, the minimum absorbed energy required in impact test is prescribed to be 2.8Kg-m at 0°C, 4.8Kg-m at −5°C and 3.6 Kg-m at −15°C for the base metal of HT50, 60 80 steels, respectively.

In this figure each minimum value prescribed by JIS or WES is shown by the broken line as "Lowest limit". As compared with those prescribed values, the absorbed energy for some of HT60 welds in (A) type fracture mode showed the value less than JIS' limit, however the value of absorbed energy for the welds of HT50 and 80 steels is exceeding the lowest limit in JIS and WES Specifications even in case of (A) type fracture modes. On the other hand, it is natural that the absorbed energy for the welds of each material showed extremely higher value than respective lowest limit in case of (C) type.

Furthermore, in case of HT50 and 80 steels the absorbed energy for the electron-beam welds showed rather higher value than that for the submerged arc welds.

4. Conclusion

Nondestructive inspection, hardness distribution, and impact properties of weld metal were made clear on the electron-beam welds for three commercial high tension steels (HT50, 60 and 80). The results obtained were as follows:

(1) Defect of welds

According to X-ray inspection for the electron-beam welds, hot cracks were often observed in the crater points, or the plasces where the electron beam irregularily stopped due to arcing etc.. However, in accordance with JIS Specification most of electron-beam welds except irregular points were allowable in the first class

Table 3 Relation between weld heat input and transition temperature for fracture mode in various materials.

Steel	Weld heat input (KJ/cm)	Transition temperature for fracture mode (° C)	d_B (mm)	H_W (VHN)	d_B/h	H_W-H_S/H_S
HT50-weld metal	10	−60	1.2	323	0.15	0.96
	15	−15	2.6	280	0.33	0.70
	20	−15	2.6	259	0.33	0.57
	40	> 15	3.3	196	0.41	0.19
HT60-weld metal	10	−40	1.2	349	0.15	0.59
	20	−15	2.6	293	0.33	0.33
	40	15	3.3	247	0.41	0.12
HT80-weld metal	10	−40	1.2	420	0.15	0.58
	15	−40	2.6	402	0.33	0.52
	40	−15	3.3	342	0.41	0.29

d_B: Bead width at 7 mm depth from surface
h: Remaind length of Charpy 2 mm-Vnotch specimen, 8mm
H_W: Average hardness of weld metal, VHN
H_S: Average hardness of base metal or HAZ, VHN
(HT50; H_S=165, HT60: H_S=220, HT80; H_S=265)

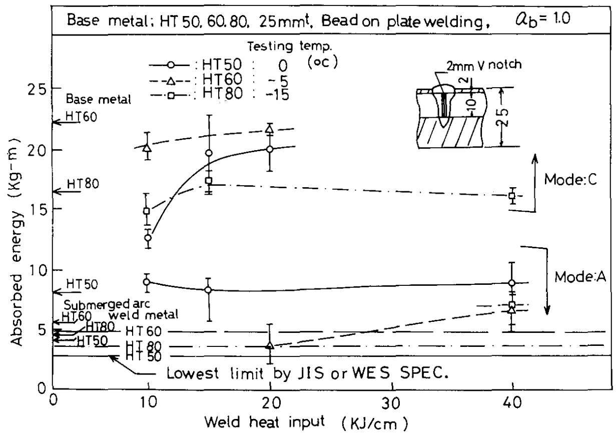

Fig. 12 Relation between weld heat input and absorbed energy of weld metal at specified temperature in JIS or WES Specification for various materials.

for synthetic grade. And also there were no surface defects in dye penetrant test.

As a result it was found that particular cares should be taken for crater treatment and not to beam-stop irregularily due to the arcing for electron-beam welder in order to obtain perfect welds.

(2) Hardness examinations

(i) The hardness of weld metal are gradually decreased with an increase of the weld heat input.
(ii) In the hardness distributions of weld metals inward direction for HT50 and 60 welds, the tops of spiking showed the maximum value of hardness.
(iii) The softened zones were observed in the hardness distribution of HT60 and 80 welds.

(3) Impact properties

(i) There were not particular variations in the impact strengths of the weld metal in itself within the changing range of weld heat input in this investigation. And in case of HT50 welds the value of them corresponded to that of the base metal, but in case of HT60 and 80 welds it was remarkably lower than that.
(ii) In general, the value of impact strength for the weld metal showed the different levels at the particular testing temperature due to the difference in the fracture mode. And at lower temperature, the absorbed energy showed the low value, as the fracture occurred straightly along the notched direction, however at higher temperature it showed the high value as the fracture occurred out of the notched direction.
(iii) The transition temperature for fracture mode in general tends to shift to higher temperature with an increase of the weld heat input.
(iv) It was found that the transition temperature for fracture mode was closely related to both the bead width and the hardnened degree of weld metal.
(v) As compared with the minimum abosrbed energy for respective base metal prescribed by JIS or WES Specification, in some of HT60 welds, the absorbed energy of the weld metal in itself showed the value less than JIS' limit. However in HT50, HT80 and the other HT60 welds it is exceeding the lowest limit in JIS and WES Specifications. And as compared with submerged arc welds, in case of HT50 and 80, the absorbed energy for electron-beam welds showed rather higher value than that for them.

Acknowledgement

Sincere appreciation is expressed to Mr. T. Kojima, Katayama Iron Works, Ltd. and Mr. S. Katayama the graduate student of the Welding Department, Osaka University, who kindly assisted us for carring out the various tests.

References

(1) Y. Arata, F. Matsuda, Y. Shibata, S. Hozumi, Y. Ono and S. Fujihira, "Mechanical Properties on Electron Beam Welds of Constructional High Tension Steels (Report I)", Trans. of JWRI, Vol 3, No. 2,59～74, 1974.
(2) Y. Arata, F. Matsuda, Y. Shibata, S. Hozumi, Y.Ono and S. Fujihara. "Mechanical Properties on Electron Beam Welds of Constructional High Tension Steels((Report II)," Trans. of JWRI, Vol.4, No. 1,65～69, 1975
(3) Y. Arata, K. Terai and S. Matsuda, "Study on Characteristics of Weld Defect and Its Prevention in Electron Beam Welding (Report I)", Trans. of JWRI, Vol. 2, No. 1,103～112, 1973.